Exploring Chemical Reactivity through a combined Conceptual DFT and ELF Topology Approach

Bastien Courbière, Julien Pilmé

Exploring Chemical Reactivity through a combined Conceptual DFT and ELF Topology Approach

Bastien Courbière[1] and Julien Pilmé[1*]

[1]Sorbonne Université, CNRS,, Laboratoire de Chimie Théorique, 4, place Jussieu, Paris Cedex 05, 75052, France.

*Corresponding author(s). E-mail(s): julien.pilme@sorbonne-universite.fr;
Contributing authors: bastien.courbiere@sorbonne-universite.fr;

Abstract

Context In a proof-of-concept study, we explore how a combined approach using the topology of the Electron Localization Function (ELF) and the condensed Dual Descriptor (DD) function can guide the optimal orientation between reactants and mimic the potential energy surfaces of molecular systems at the beginning of the chemical pathway. The DD has been chosen for its ability to evaluate the regioselectivity of neutral and soft species, and to potentially mimic the interaction energy obtained from the mutual interactions between nucleophilic and electrophilic regions of the building blocks under perturbative theory.
Method Our method has been illustrated with examples that show the optimal orientation of several systems can be successfully identified. The limitations of the presented model in predicting chemical reactivity are outlined in particular the influence of the selected condensation scheme.

Keywords: Chemical Bond, Density Functional Theory, Lewis Structure, Dual Descriptor, Quantum Chemical Topology, ELectron localization function

Introduction

In the early stages of a complex reaction pathway, the driving forces often depend on charge transfer contributions, which can overtake the coulombic terms when the reactants are far apart. This statement has long been used to predict reactivity. For

example, the Klopman-Salem model summarizes this interacting view well and considers a chemical reaction to be either driven by charge-charge contributions or interacted by orbital overlap.[1–3]. This has also led to some new concepts such as the HSAB principle or the maximum hardness and minimum electrophilicity rules. [4–6] Afterwards, an unified perturbative view through the conceptual DFT (cDFT) was proposed, offering a rigorous method to describe the reactivity between reactants. [7–9] The cDFT point of view considers the flow of electrons from the species with a higher chemical potential (donor) to the one with a lower chemical potential (acceptor) to balance the two chemical potentials according to Sanderson's principle in the new interacting system. [10, 11]. This process may be dominant for species with a small gap between their highest occupied molecular orbitals (HOMO) and their lowest unoccupied molecular orbitals (LUMO). The Frontier Molecular Orbital (FMO) theory, originally proposed by Fukui, is derived from this concept. [12, 13] Over the past few decades, Fukui functions and the so-called Dual Descriptor have become invaluable tools for elucidating chemical mechanisms and gaining insight into reactivity by identifying electrophilic and nucleophilic regions within the molecular space. [14–17]

In the meantime, alternative strategies for rationalizing the interactions between atoms or molecules based on non-overlapping interacting topological domains have emerged from the pioneering works of Richard Bader in the 1970s. [18, 19] The Interacting Quantum Atoms (IQA) energy approach, when applied to the QTAIM partition [20] or more recently to the electron localization function (ELF) [21–23], provides an alternative scheme to rationalise chemical reactivity and identify the most favourable relative orientations between reactants beyond the FMO approximation. [**?**] These include the behaviour of condensed Fukui functions or DD over topological domains.[24–27] In line with these works, this study presents a new way for identifying the electrophilic and nucleophilic ELF topology domains of reactants and how they interact to predict the regioselectivity.

Theory

Quantum Chemical topology

It is assumed that the reader is already familiar with the quantum chemical topology (QCT), as many papers have been published in the litterature.[19, 28] In short, QCT is dedicated to answering general questions about chemical bonding in molecules and solids. QCT is based on the theory of gradient dynamical systems, which allows the partitioning of molecular space into basins. The most commonly used is the electron density, giving rise to the quantum theory of atoms-in-molecules (QTAIM).[29, 30] Since these basins are only atomic, a topological atom can be defined as the union of a nucleus with its associated electron density basin. Another widely used function is the electron localisation function (ELF), which is usually interpreted as a signature of the distribution of electron pairs in molecular space.[22] The ELF topology depicts some non-atomic valence basins in addition to valence and nuclear basins surrounding nuclei with atomic number Z$>$ 2. In all cases the basins are bounded by zero-flux surfaces, and integration of the electron density over each basin directly provides the corresponding population.

Recently, one of us proposed a modified ELF function designed to combine ELF with the Fukui partition of the molecular space. [31] The topological domains are the ones of the modified ELF, termed ELF_x defined from the ELF kernel as follows:

$$\mathrm{ELF}_x(\mathbf{r}) = \frac{1}{1 + \left(\frac{\chi(\mathbf{r})}{2x(\mathbf{r})}\right)^2} \tag{1}$$

The kernel $\chi(\mathbf{r})$ of ELF being usually defined as:

$$\chi(\mathbf{r}) = \frac{\tau(\mathbf{r})_N - \frac{1}{8}|\nabla\rho(\mathbf{r})_N|^2/\rho(\mathbf{r})_N}{c_F\ \rho(\mathbf{r})_N^{\frac{5}{3}}} \tag{2}$$

where $c_F = \frac{3}{10}(3\pi^2)^{\frac{2}{3}}$ is the Fermi constant, $\tau(\mathbf{r})_N$ is the positive definite kinetic energy density, and $\rho(\mathbf{r})_N$ is the total electron density of a molecular system with N electrons. $x(\mathbf{r})$ is a normalized dimensionless quantity defined in the FMO context as follows :

$$x(\mathbf{r}) = \frac{\rho(\mathbf{r})_{\mathrm{HOMO}}}{\rho(\mathbf{r})_N} \quad \text{or} \quad x(\mathbf{r}) = \frac{\rho(\mathbf{r})_{\mathrm{LUMO}}}{\rho(\mathbf{r})_{N+1}} \tag{3}$$

$\rho(\mathbf{r})_{N+1}$ is the total electron density of the molecular system with $N+1$ electrons with the same geometry and the same orbitals that are obtained for the system with N electrons. In summary, ELF_x is a measure of electronic localization limited to Fukui domains.

The Dual Descriptor condensed scheme

We are interested in ambiphilic systems that can act as nucleophiles and electrophiles simultaneously, depending on the reaction partner. Within the cDFT, an appropriate response function can be the Fukui functions, which are defined as the variation of the chemical potential under variation of the external potential at a fixed number of electrons. Another response function is the Dual Descriptor for chemical reactivity, which has been used, for example, for Diels-Alder reactions and to rationalize the rules of Woodward and Hoffmann.[32] The Dual Descriptor $f^{(2)}(\mathbf{r})$ is a local function defined as the first derivative of Fukui functions with respect to the number of electrons at a fixed external potential.

$$f^{(2)}(\mathbf{r}) = \left(\frac{\partial f(\mathbf{r})}{\partial N}\right)_{v(\mathbf{r})} \tag{4}$$

where $f(\mathbf{r})$ is a Fukui function. In the finite difference approximation, eq (4) can be rewritten as :

$$f^{(2)}(\mathbf{r}) = f^{+}(\mathbf{r}) - f^{-}(\mathbf{r}) \tag{5}$$

where $f^{+}(\mathbf{r})$ and $f^{-}(\mathbf{r})$ are the right- and left-hand-side Fukui functions. High values of Fukui indicate the most favorable regions to receive or donate electrons characterizing sites of high electrophilicity or nucleophilicity, respectively. Commonly, the FMO

approximation can be used to obtain a simple expression for the Fukui function :

$$f^{-}(\mathbf{r}) \approx |\phi(\mathbf{r})_{HOMO}|^2 \text{ and } f^{+}(\mathbf{r}) \approx |\phi(\mathbf{r})_{LUMO}|^2 \tag{6}$$

where $\phi(\mathbf{r})$ is the molecular orbital. Unfortunately, these expressions are known to fail for degenerate or quasidegenerate states. Interestingly, a orbital-weighted scheme was recently proposed by Pino-Rios et al. in order to prevent the degenerate frontier orbitals cases [33, 34] :

$$f^{-}(\mathbf{r}) \approx \sum_{i=1}^{HOMO} w_i^o \ |\phi_i(\mathbf{r})|^2 \text{ and } f^{+}(\mathbf{r}) \approx \sum_{i=LUMO}^{\infty} w_i^v \ |\phi_i(\mathbf{r})|^2 \tag{7}$$

where w_i are the weights running over a set of molecular orbitals defined according to an ansatz gaussian strategy as :

$$w_i^o = \frac{exp\Big(-\big(\frac{\mu - \epsilon_i}{\Delta}\big)^2\Big)}{\sum_{j=1}^{HOMO} exp\Big(-\big(\frac{\mu - \epsilon_i}{\Delta}\big)^2\Big)} \text{ and } w_i^v = \frac{exp\Big(-\big(\frac{\mu - \epsilon_i}{\Delta}\big)^2\Big)}{\sum_{j=LUMO}^{\infty} exp\Big(-\big(\frac{\mu - \epsilon_i}{\Delta}\big)^2\Big)} \tag{8}$$

where μ, ϵ_i and Δ are the chemical potential, the orbital energy and the width of the Gaussian function, respectively. The width parameter adjusts contributions from various frontier orbitals. As one moves away from the frontier orbital levels, the weights decrease due to Gaussian weighting. Note that perfect degeneracy is still accounted for, as equal weights are assigned to degenerate levels. Although the choice of Δ is non-trivial, Equations (7) and (8) provide a useful approach for evaluating the Fukui functions and the Dual Descriptor when degeneracy occurs. Typically, a value Δ=0.01 (or 0.02) is suitable for most of cases.

Although nucleophilic/electrophilic sites in molecules can often be easily identified by a simple examination of 3D isosurfaces of the DD function, quantitative details such as the location of DD extrema are more difficult to extract. Interestingly, local information can be summarized in terms of reactive sites by condensing reactivity descriptors. Previous schemes such as QTAIM and Hirshfeld condensation schemes have been proposed with limited success to quantitatively predict stereoselective reactive tendencies. [25] A major concern is that reactivity sites between reactants are mostly non-atomic and need to be assigned as a signature of the distribution of electron pairs in order to play a role related to chemical reactivity. The ELF or ELF$_x$ topologies being mostly non-atomic, they can be used in that way. The condensed Dual Descriptor over the ELF or ELF$_x$ ($CEDD$), reads as follows :

$$\bar{N}_{CEDD} = \int_{\Omega} f^{(2)}(\mathbf{r}) \ d\mathbf{r} \tag{9}$$

Over the whole molecular space the property $\sum_{\Omega} \bar{N}_{CEDD} = 0$ need to be filled. As shown in Figure 1 each domain Ω can be assigned to a nucleophilic/electrophilic character in the following way :

1. $\mathbf{\bar{N}_{CEDD} > 0}$: The average of DD over the volume of the basin is positive, which can be interpreted as a local electrophilic character for the targeted domain.
2. $\mathbf{\bar{N}_{CEDD} < 0}$: The average of DD over the volume of the basin is negative, which can be interpreted as a local nucleophile character for the targeted domain.
3. The absolute value of $\bar{N}_{CEDD}$ remains close to zero. Either most of the values integrated into the domain are small, or there is a compensation between positive and negative values. Either way, the domain displays an aphilic character. The ELF core basins C(A) have typically a tagged aphilic character.

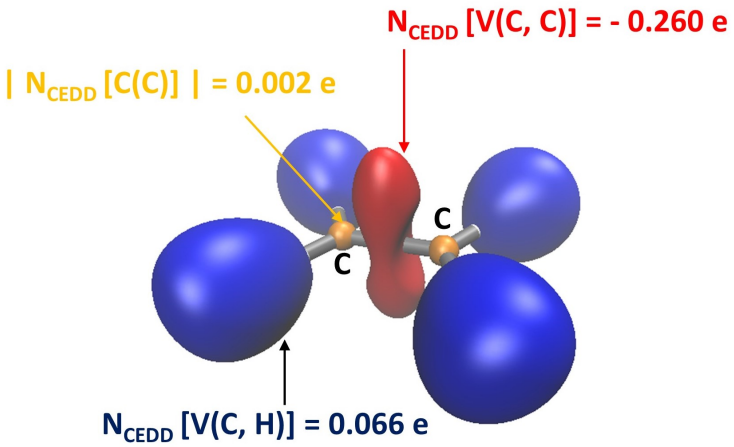

Fig. 1 ELF localization domains of the C_2H_4 molecule optimized at the wb97xd/cc-pvtz level of theory. Color Code : red: V(C, C) nucleophilic domains, blue: V(C, H) electrophilic domains, core C(C) orange : aphilic domains

Interacting descriptor based-on the condensed ELF Dual Descriptor (EDD)

When a donor MA meets an acceptor species MB, they begin to interact (we assume that the deformation energies of the fragments can be neglected), the coulombic contributions can typically be overtaken by the charge transfer contributions, which largely contribute to the driving force. They have proven their efficiency in determining the nucleophilic and electrophilic key domains of interacting reactants under orbital control, and should be able to describe the energetic changes that occur between the reactants. From this point of view, a global bielectronic descriptor EDD can be defined as follows :

$$EDD = \sum_A \sum_B \int_{\mathbf{r}_1 \in \Omega_A} \int_{\mathbf{r}_2 \in \Omega_B} \frac{f^{(2)}(\mathbf{r}_1)\ f^{(2)}(\mathbf{r}_2)}{|\mathbf{r}_1 - \mathbf{r}_2|}\ d\mathbf{r}_1\ d\mathbf{r}_2 \tag{10}$$

Where Ω_A and Ω_B are the domains of MA and MB, respectively. EDD depends entirely on the relative orientation between the "frontier" densities of molecular fragments and it can be used to predict the regioselectivity of systems like clusters. Note that EDD can be related to the maximum matching criterion previously defined in terms of Fukui functions in the whole molecular space. [35]

Practical computation of EDD

The practical calculations of Eq 10 requires a enough heavy computational cost not really appropriated for practical applications. However, it can be numerically evaluated by means of a multipole expansion (ME). The latter needs accurate computations of charge distributions at any point of the molecular space. The ME is based on a Taylor expansion of the $|r_1 – r_2|$ - 1 term, which leads to well-known form :

$$\sum_{l_A=0}^{\infty}\sum_{l_B=0}^{\infty}\sum_{m_A=-l_A}^{l_A}\sum_{m_B=-l_B}^{l_B} T_{l_A,l_B,m_A,m_B}(R_{AB})\; Q_A^{\Omega}(m_A,l_A)\; Q_B^{\Omega}(m_B,l_B) \tag{11}$$

where $\mathrm{T}_{l_A,l_B,m_A,m_B}$ is an interaction tensor obtained from stable recurrence relations. The indexes are computed $\mathrm{l}_{A/B}$ and $\mathrm{m}_{A/B}$ are the distributed multipole moments on the topological partition. Using only the first terms of the ME $\bar{N}_{CEDD}$ (that is only the monopoles) and considering Eq.10, EDD reads as follows:

$$EDD \approx \sum_A \sum_B \frac{\bar{N}_{CEDD}^A\; \bar{N}_{CEDD}^B}{|R_A - R_B|} \tag{12}$$

Where $R_{A/B}$ are the locations of basin attractors belonging to Ω_{ELF} domains of MA and MB, respectively. Note that Eq.12 does not restricted to just two reactants but could be used for complex mechanisms involving several reactants.

Limitations of the proposed methodology

If only aphilic domains are found in a given fragment, Eq.12 becomes unworkable. This may be the case for monoatomic systems (e.g. Cl^- anion) where condensed electrophlic and nucleophilic contributions are compensated each other. The method is also, by definition, limited to the usual perturbative scheme of cDFT, especially considering that the charge transfer is small and deformation energies of fragments (variation of the external potential) should be also small. This usually refers to intermolecular interactions between systems that are far apart.. The preferred regioselectivity between donor/acceptor systems is suitable for non-covalent compounds such as clusters or hydrogen-bonded systems. However, a purpose of this work is also to open up the ability of the descriptor towards the chemical reactivity in a more general way at early stages of the reaction. Note that the choice of the condensed scheme over a real-space electron domain remains arbitrary as long as the definition of an atom in a molecule remains arbitrary. Thus, the influence of a given condensation scheme (choice of topological partition) on the results need also to be investigated. [26]

Methods

The $\omega B97XD$ long-range corrected functional [36] level with the Gaussian 16 [37] software has been used to perform all the calculations, with a standard all-electron aug-cc-pVTZ basis for all atoms. [38]. The D2 version of Grimme dispersion model [39] has also been used to heed the Van der Waals interactions in the studied systems. Each minima displays only positive eigenvalues. We considered only the single states for each geometry and checked that the results correspond to a minimum. The condensation of DD over the ELF basins have been performed using the TopChem2 program package. [40, 41]. This package incorporates specific parameters, including variations of sizes for the parallelepipedic box, steps between the grid points along with precision levels for the computation of the orbital-weighted Fukui function [33].

Results and discussion

Selected Systems

For the sake of simplicity, we restrict ourselves in this paper to the interaction between two closed-shell reactants. Note that the proposed methodology could easily be extended to multiple reactants or open-shell systems which could be presented in a future study. We explored the conformational space of the interacting fragments MA (donor) + MB (acceptor) $\rightarrow MA--MB$, seeking extrema on the potential energy curves of EDD. The applicability of EDD has been evaluated in several examples, as detailed in Figure 2. Firstly, we considered monomers bound by non-covalent interactions, including the canonical dimer water, the donor-acceptor NH_3-H_2S system, the typical hydrogen bond FH—CO/OC systems and the guanine-cytosine pair. The methodology was also evaluated for the characterization of the Bürgi-Dunitz Angle. Additionally, a reactive process was considered with the Diels Alder mechanism involving $C_2H_4 + C_4H_6 \rightarrow$ Cyclohexene. In order to ascertain the suitability of the descriptor for predicting the regioselectivity, a series of rotation schemes between reactants were examined and shown in Figure 2. The geometries of fragments were frozen and maintained at their isolated geometries in all calculations. To ensure clarity of the analysis, all the curves were displayed as normalized plots $\frac{f-min(f)}{max(f)-min(f)}$ where f is the studied function namely f $\equiv$ DFT interaction energy or f $\equiv$ EDD.

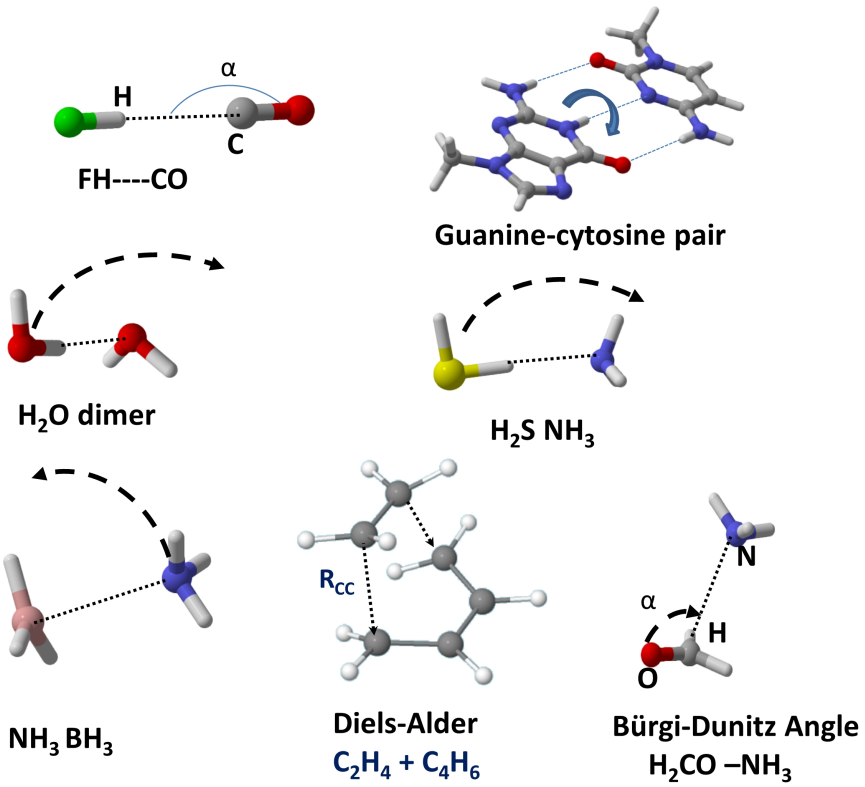

Fig. 2 Selected Compounds and the applied rotation schemes. For Diels-Alder, we considered the two fragments C_2H_4 and C_4H_6 approaching one another

Condensed Dual Descriptor over the ELF domains

Table 1 presents the $\bar{\mathbf{N}}_{\mathbf{CEDD}}$ obtained using the ELF basins for a selected set of molecules. Overall, the condensed values are consistent with the local reactivity for both donor and acceptor species. More specifically,

1. A core basin C(A) is typically aphilic, sincde the condensed DD over the volume basin is close to zero. They may occasionally exhibit a small electrophilic or nucleophilic character, depending on the chemical environment. Overall, the core basins contribute a very small amount to EDD, which is consistent with the chemistry point of view where reactivity is mainly driven by the valence environment. It is noteworthy that the case of BH_3 represents an exception. This electrophilic species exhibits only three protonated valence V(H, B) basins, which display an aphilic character ($\bar{\mathbf{N}}_{\mathbf{CEDD}}$=-0.007e). Consequently, only the core basin C(B) exhibits a local electrophilic character consistent with the well-known electron deficiency of this species.
2. The protonated domains V(A, H) are almost invariably electrophilic except for the O-H bond in Phenol which exhibits a nucleophilic character. This is consistent with

Table 1 $\tilde{\mathbf{N}}_{\mathbf{CEDD}}$ (electrons) for some molecules computed at the wb97xd/cc-pvtz level of theory. $\Delta = 0.01$ was used as indicated in the reference [33]

Molecules	Core	Non-bonding	Protonated bond	Covalent bond
C_2H_4	C(C) 0.002		V(C, H) 0.066	V(C, C) -0.130
C_4H_6	C(C) 0.001		V(C, H) 0.029	V(C, C) -0.071/-0.058/0.093
C_6H_6	C(C) 0.000		V(C, H) 0.022	V(C, C) -0.022
C_6H_6O	C(C) 0.008		V(C, H) 0.052	V(C, C) -0.047/-0.027/0.052
	C(O) -0.01	V(O) -0.077	V(O, H) -0.016	V(C, O) -0.010
CO $^(a)$	C(C) 0.006	V(C) -0.046		V(C, O) -0.025
	C(O) 0.004	V(O) 0.061		
H_2CO	C(O) -0.014	V(O) -0.159	V(C, H) 0.083	V(C, O) 0.140
N_2	C(N) 0.001	V(N) 0.006		V(N, N) -0.014
HCN	C(N) -0.001	V(N) 0.043	V(C, H) 0.229	V(C, N) -0.277
NH_3	C(N) -0.029	V(N) -0.501	V(N, H) 0.177	
H_2O	C(O) -0.032	V(O) -0.288	V(O, H) 0.231	
H_2S	C(S) -0.025	V(S) -0.215	V(S, H) 0.228	
FH	C(F) -0.023	V(F) -0.606	V(F, H) 0.629	
BH_3	C(B) 0.020		V(B, H) -0.007	
BF_3	C(B) 0.047	V(F) -0.132		V(B, F) 0.125

the well-known nucleophilic behaviour of ortho-carbon atoms and the oxygen lone pairs in the electrophilic aromatic substitutions. [42]

3. Overall, the bonding covalent domains V(A, B) show a nucleophilic character. Note that the C-O bond in H_2CO is expected electrophilic due the strong contribution of the polarized C^+ O^- scheme.
4. The non-bonding domains are typically nucleophilic. The case of CO is noteworthy because of its ambivalent nature. A higher value of Δ (=0.05) than usual was used because the reactivity depends on both HOMO-1 and HOMO-2 orbitals. [43] *CO* is a C-nucleophilic agent where $\tilde{\mathbf{N}}_{\mathbf{CEDD}}$ for V(C) was consistently found negative (-0.046e). This is mainly due to the pivotal role of the σ HOMO orbital. In contrast, V(C, O) and V(O) show an electrophilic character, which is unusual. In fact, this is consistent with the Dewar-Chatt-Duncanson balance [44] (σ-donation to Metal and π^*-back-donation from Metal), which is an organometallic chemistry model explaining, for example, the chemical bonding in transition metal alkene complexes.

Non-covalent Interactions

Let us consider non-covalent systems for which the charge transfer between monomers is expected to be small and the geometries of reactants are expected to be weakly modified.

Dimer hydrogen-bonded systems

We start with two archetypal hydrogen bonding systems: the water dimer and the H_2S-NH_3 dimer. Figure 3 shows a comparative study of the variation of *EDD* vs. the DFT intermolecular interaction energy. The hydrogen bond between the electrophilic protonated basin V(O, H)/V(S, H) and a nucleophilic lone pair V(O)/V(N) is expected

to be the significant interaction. Rotations of H_2O or H_2S around the other monomer have been performed retaining the hydrogen bonding schem"e for each configuration. As observed in Figure 3, the optimal orientation of the reactants is associated with the lowest value of EDD and a faithful mapping of EDD and the DFT intermolecular interaction energy curves is observed.

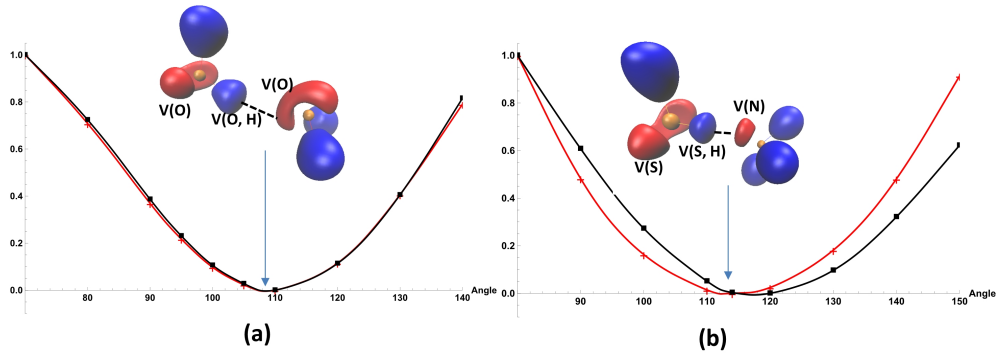

Fig. 3 ELF localization domains and comparative study of the normalized variation of EDD (black) v.s. the DFT intermolecular interaction energy (red). Color code : red nucleophilic basins and blue electrophilic basins. The orientation of monomers is displayed in Figure 2 (a) Rotation of the water monomer around the other water molecule (mass centers of reactants separated from 3 Å (b) Rotation of the H_2S monomer around the NH_3 molecule (mass centers of reactants separated from 3 Å). The geometries of reactants is constrained to that obtained in their isolated states.

FH-CO/OC hydrogen-bonded dimers

The case of the weakly bound dimer complexes FH–CO and FH–OC is examined. At the DFT level of theory, both complexes exhibit a minimum, with FH–CO being the most stable. Figure 4 displays the DFT plot (red curve) associated with the rotation of CO ($^1\Sigma^+$) around the center of mass of the FH ($^1\Sigma^+$) molecule. The curve shows two minima for $\alpha = 0^o$ (FH-CO, global minimum) for $\alpha = 180^o$ (FH-OC, local minimum). A maximum is observed for $\alpha = 90^o$ where the CO fragment is perpendicular to the FH fragment. The variation of EDD (black curve) is also displayed in Figure 4. The global minimum observed on the EDD plot (FH-CO) is in excellent mapping with the related DFT curve. In contrast, EDD highlights a local maximum associated with the FH-OC structure. As previously discussed, the C-O π^* bond and the oxygen site are associated with an electrophilic behavior (EDD >0), leading to a repulsive interaction with the hydrogen of the FH moiety. In fact, the reactivity of the oxygen site seems to be characterised by its negative charge rather than an orbital character described by the Dual Descriptor. [45]

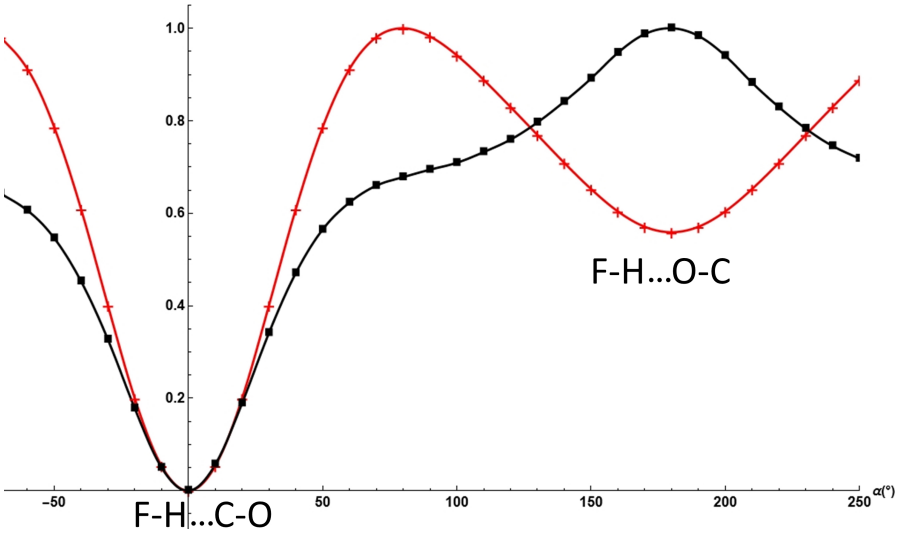

Fig. 4 Comparative study of the normalized variation of ELF EDD (black) v.s. the DFT intermolecular interaction energy (red) for the rotation of the CO species around the FH molecule (mass centers of reactants separated from 3 Å). The geometries of reactants are constrained to that obtained in their isolated states and their orientations are displayed in Figure 2.

The Cytosine-Guanine pair

Let us consider the hydrogen bonds that hold guanine–cytosine (GC) pair as depicted in Figure 2. The main concern evaluated in this section relates to the validity of the methodology regarding the relative orientation of the Watson-Crick base pair system, where hydrogen bonds play a crucial role in the stability of the system. This is clearly related to a charge-transfer due to orbital interactions (oxygen and nitrogen lone pairs and N-H σ^* character). [46, 47] Figure 5 displays the obtained EDD plot together with the corresponding plot of the DFT intermolecular interaction energy computed for the rotation of the cytosine molecule around the guanine molecule taken in their respective isolated states. Once again we observe a very good mapping of EDD onto the DFT profile. Indeed, the location of the global minimum is the same and correspond to the well known orientation between Cytosine and Guanine leading to the natural Watson Crick base pair GCWC structure where three typical HNH—O=C/NH—N/C=O—HNH intermolecular hydrogen bonds are observed.

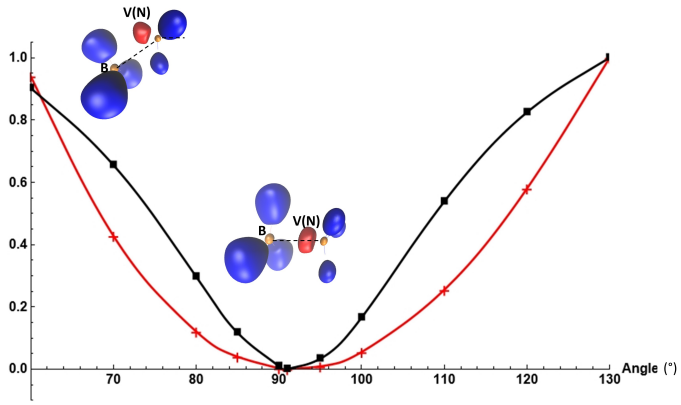

Fig. 5 Comparative study of the normalized variation of EDD (black) v.s. the DFT intermolecular interaction energy (red) for the cytosine-guanine pair. The orientation of monomers is displayed in Figure 2. Rotation of the cytosine around the guanine molecule (mass centers of reactants separated from 3 Å). The geometries of reactants is constrained to that obtained in their isolated states (see Figure 2).

Prediction of the Bürgi-Dunitz Angle

The Bürgi-Dunitz angle is related to the addition of a nucleophilic compound on an unsaturated electrophilic carbon, originally in the organic ketones, but later identified with aldehydes, esters, amide carbonyls as well as alkenes.[48–52] The mechaninistic process involves the FMO approximation for both interacting compounds. In the case of an attack on a carbonyl, the $HOMO$ orbital is typically a p type orbital and the $LUMO$ is typically an anti-bonding π^* orbital perpendicular to the plane containing the C=O bond and its substituents. The value of the angle depends on the system, but it is generally lower than 120^o.

We have selected a typical system of the NH_3 for the nucleophilic species interacting with H_2CO. Figure 6 displays the comparative study of the variation of EDD v.s. the DFT intermolecular interaction energy where several values of the Bürgi-Dunitz angle have been tested. At the DFT level of theory, the optimal angle is found to be close to 115^o (red curve). Conversely, the EDD curve does not exhibit any minimum. The reason of this finding is relatively straightforward to identify. As shown in Figure 6 (green plot), the condensed DD over the ELF topological domains for H_2CO does not show any specific non-atomic domain opposite to the nitrogen lone pair. In contrast, using the ELF_x partition for H_2CO (black plot), we can identify two specific electrophilic ELF_x domains opposite to the nucleophile. In this case the EDD plots show a minimum angle close to 108^o in good agreement with the DFT value. This example clearly illustrates the effect of the choice of topology used for the condition scheme on the predictions made for the reactivity of molecular systems.

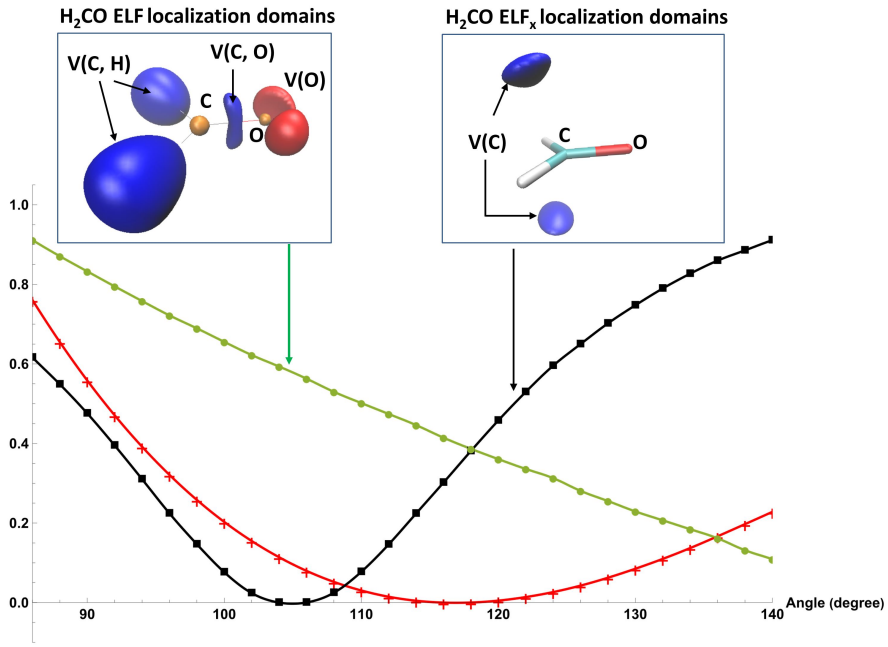

Fig. 6 Comparative study of the normalised variation of EDD (black and green) v.s. the DFT intermolecular interaction energy (red) for the Bürgi-Dunitz NH_3-H_2CO system computed at the wB97XD/cc-pVTZ level of theory. Color code : black: ELF condensed domains for NH_3 and ELF_x condensed domains for H_2CO ; green : ELF condensed domains for both NH_3 and H_2CO. Red/blue volumes are the nucleophilic/electrophilic domains, respectively.

The case of a dative interaction : the archetypal NH_3BH_3

Regarding the formation of borazane NH_3BH_3, the equilibrium structure exhibits a B-N distance near 1.65 Å . Its chemical path has long been known, the bond formation coming from a strong electron transfer between the HOMO of NH_3 and the LUMO of BH_3 as an archetypical strong Lewis acid-base mechanism (dative bond). [27, 53] As illustrated in Figure 2, the optimal charge transfer is associated with a typical structure where the nitrogen lone pair is perfectly oriented in front of the boron-depleted site (α=90^o). In this study we want to determine whether the descriptor is able to identify this preferred orientation of the NH_3 molecule relative to the BH_3 fragment as shown in Figure 2. The conformational space of the rotation of NH_3 around BH_3 was explored in the range between α=[70^o -130^o] and we looked for the minima of the EDD curve. Once again, Figure 7 shows a noticeable mapping of the EDD curve onto the DFT energy curve, with the location of the minimum being close to 90^o for the both plots.

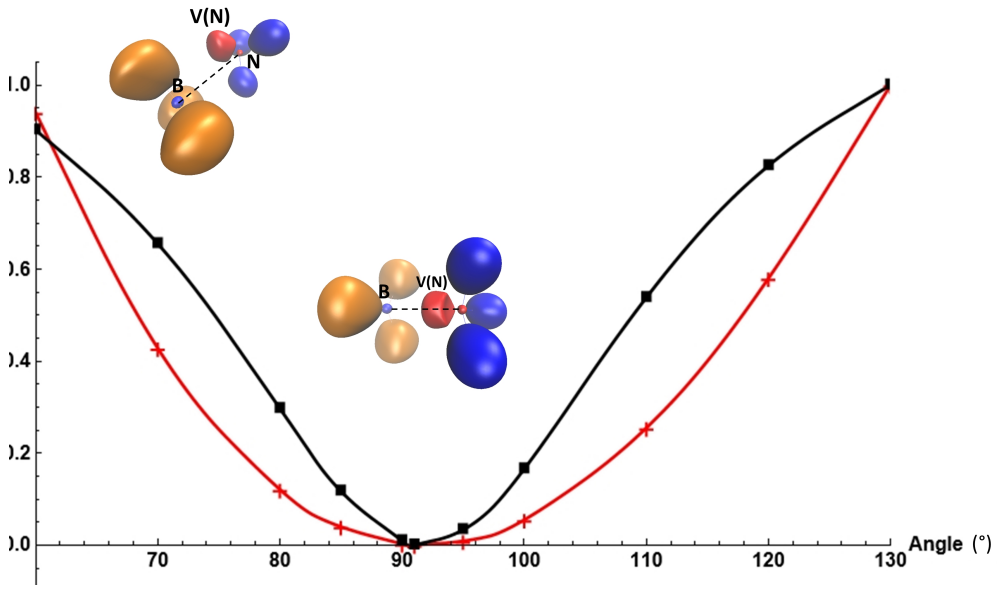

Fig. 7 Comparative study of the normalised variation of EDD (black) v.s. the DFT intermolecular interaction energy (red) for the NH_3-BH_3 system computed at the wB97XD/cc-pVTZ level of theory. ELF localization doamins Color code : red : nucleophilic basins, blue: electrophilic basins and orange: aphilic basins. The orientation of monomers is displayed in Figure 2 Rotation of the NH_3 fragment around the BH_3 (mass centers of reactants separated from 3 Å). The geometries of reactants is constrained to that obtained in their isolated states

Towards Chemical Reactivity : Diels Alder (DA) reaction

Although the applicability field of EDD is expected to be rather restricted non-covalent systems, we can explore its ability to describe and predict the topology of the potential energy curves at the beginning of reaction paths. This has been achieved through a pericyclic concerted Diels-Alder reaction, which illustrates the presence of a kinetic barrier. This reaction has been widely used in synthetic organic chemistry for carbon-carbon bond formation and plays a central role in the development of theoretical models of pericyclic mechanisms. [54, 55] The reaction between ethylene and 1,3-butadiene to yield cyclohexadiene is often cited as a textbook example. Figure (8) shows a comparative study of the normalized variation of EDD v.s. DFT according to the RCC distances (see Figure 2. The challenge is to test whether the approach can accurately reproduce the activation barrier. As shown in Figure (8), EDD closely aligns with the DFT plot, which gradually rises from the large distances R_{CC} to a saddle-point observed for EDD at $R_{CC} \approx 2.3$ Å. This latter distance is very close to the DFT value of 2.2 Å. These results show that EDD can reasonably describe a chemical process that encompasses a transition state which occurs early along the reaction path, extending beyond a straightforward associative process where no kinetic barrier is involved.

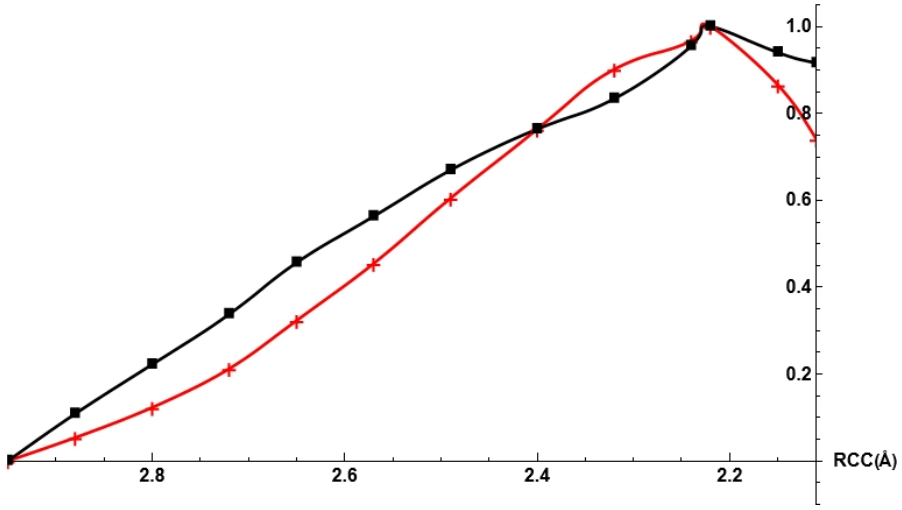

Fig. 8 Comparative study of the normalized variation of EDD (black) v.s. the DFT intermolecular interaction energy (red) for the Diels-Alder reaction C_2H_4 + C_4H_6 calculated as a function of the R_{CC} coordinate.

Conclusions and Outlooks

In summary, our proof-of-concept study describes an original point of view that combines both the conceptual and QCT approaches. This led to the development of an efficient scheme for predicting regioselectivity. We have shown how a condensed topological scheme can be a tractable quantity for driving chemical reactivity between reactants. Our methodology has been tested for non-covalent bonds and more generally, for donor/acceptor systems where the frontier orbitals approach is appropriated. It has also been tested with the Diels-Alder mechanism, which shows a kinetic barrier along the reaction path. Overall, our approach reveals a noticeable mimicking of EDD onto the profile of the DFT intermolecular interaction energy. However, we have shown that the approach is constrained by the choice of the topological partition, which may not be suitable for all systems. In addition, the analysis of the FHCO/OC system has shown that the identification of higher energy structures remains a challenge for further investigations. As we have presented only a few examples, future works will focus on the description and prediction of a large panel of interactions and chemical reactions. We are also currently investigating an improved expression of EDD beyond the DFT level.

Supplementary information. The online version contains supplementary material available at https://doi.org/

Author contributions. B.C. did the DFT and TopChem2 calculations, prepared the figures and wrote the Supplementary Information. J.P. wrote the main manuscript text. B.C. and J.P. conceptualization, interpretation, methodology, writing- reviewing and editing.

Funding. This research received no external funding.

Data availability. Data are available in the article and in the Supplementary Information. This latter includes additional comparative studies of the normalized variation of EDD v.s. the DFT intermolecular interaction energy together with cartesian coordinates of studied systems.

Declarations

Competing interests. The authors declare no competing interests.

References

[1] Klopman G (1968) Chemical reactivity and the concept of charge and frontier controlled reactions. J Am Chem Soc 90:223

[2] Salem L (1968) Intermolecular orbital theory of the interaction between conjugated systems i general theory. J Am Chem Soc 90:543

[3] Guégan F, Abid-Charef Y, Hoffmann G, et al (2023) Finishing (off) the klopman–salem model: the importance of density polarization energy. Theor Chem Acc 104:1432

[4] Pearson RG (1963) Hard and soft acids and bases. J Am Chem Soc 85:3533

[5] Pearson RG (1994) Principle of maximum physical hardness. J Phys Chem 98:1989

[6] Miranda-Quintana RA, Ayers PW (2018) Note: Maximum hardness and minimum electrophilicity principles. J Chem Phys 148:196101

[7] Geerlings P, De Proft F, Langenaeker W (2003) Conceptual density functional theory. Chem Rev 103:1793

[8] Geerlings, P., Chamorro E, et al (2020) Conceptual density functional theory: status, prospects, issues. Theor Chem Acc 139:s00214–020–2546–7

[9] Parr RG, Yang W (1995) Density-functional theory of atoms and molecules. Oxford University Press

[10] Sanderson RT (1951) An interpretation of bond lengths and a classification of bonds. Science 114:670

[11] Sanderson RT (1955) Partial charges on atoms in organic compounds. Science 121:207

[12] Fukui K, Yonezawa T, Shingu H (1952) A Molecular Orbital Theory of Reactivity in Aromatic Hydrocarbons. J Chem Phys 20:722–725

[13] Parr RG, Yang W (1984) Density functional approach to the frontier-electron theory of chemical reactivity. J Am Chem Soc 106:4049–4050

[14] Fuentealba P, Cárdenas C (2023) On the analysis of the fukui function. In: Kaya S, von Szentpály L, Serdaroğlu G, et al (eds) Chemical Reactivity. Elsevier, p 421–432

[15] Morell C, Grand A, Toro-Labbé A (2005) New dual descriptor for chemical reactivity. J Phys Chem A 109:205–212

[16] Guégan F, Merzoud L, Chermette H, et al (2021) A Perspective on the so-Called Dual Descriptor, John Wiley and Sons, Ltd, pp 99–112

[17] Martínez-Araya J (2015) Why is the dual descriptor a more accurate local reactivity descriptor than fukui functions? J Math Chem 53:451–465

[18] Bader RFW (1991) A quantum theory of molecular structure and its applications. Chem Rev 91:893–928

[19] Popelier PLA (2016) On Quantum Chemical Topology, Springer International Publishing, pp 23–52

[20] Guevara-Vela JM, Francisco E, Rocha-Rinza T, et al (2020) Interacting quantum atoms - a review. Molecules 25:4028

[21] Becke AD, Edgecombe KE (1990) A simple measure of electron localization in atomic and molecular systems. J Chem Phys 92:5397–5403

[22] Silvi B, Savin A (1994) Classification of chemical bonds based on topological analysis of electron localization functions. Nature 371:683–686

[23] Martín Pendás A, Francisco E, Blanco M (2008) Electron–electron interactions between elf basins. Chem Phys Lett 454:396–403

[24] Chamorro E, Duque M, Cárdenas C, et al (2005) Condensation of the highest occupied molecular orbital within the electron localization function domains. J Chem Sci 117:419–424

[25] Zielinski F, Tognetti V, Joubert L (2012) Condensed descriptors for reactivity: A methodological study. Chem Phys Lett 527:67–72

[26] Tiznado W, Chamorro E, Contreras R, et al (2005) Comparison among four different ways to condense the fukui function. J Phys Chem A 109:3220–3224

[27] Klein J, Fleurat-Lessard P, Pilmé J (2021) New insights in chemical reactivity from quantum chemical topology. J Comput Chem 42:840–854

[28] Silvi B, Gillespie RJ, Gatti C (2013) 9.07 - electron density analysis. In: Reedijk J, Poeppelmeier K (eds) Comprehensive Inorganic Chemistry II (Second Edition), second edition edn. Elsevier, Amsterdam, p 187–226

[29] Bader RFW (1991) A quantum theory of molecular structure and its applications. Chem Rev 91:893–928

[30] Popelier PLA (2014) The QTAIM Perspective of Chemical Bonding, John Wiley Sons, Ltd, chap 8, pp 271–308

[31] Pilmé J (2017) Electron localization function from density components. J Comput Chem 38(4):204–210

[32] Geerlings P, Ayers PW, Toro-Labbé A, et al (2012) The woodward–hoffmann rules reinterpreted by conceptual density functional theory. Acc Chem Res 45:683–695

[33] Pino-Rios R, Yañez O, Inostroza D, et al (2017) Proposal of a simple and effective local reactivity descriptor through a topological analysis of an orbital-weighted fukui function. J Comput Chem 38:481–488

[34] Pino-Rios R, Inostroza D, Cárdenas-Jirón G, et al (2019) Orbital-weighted dual descriptor for the study of local reactivity of systems with (quasi-) degenerate states. J Phys Chem A 123(49):10556–10562

[35] Osorio E, Ferraro MB, Oña OB, et al (2011) Assembling small silicon clusters using criteria of maximum matching of the fukui functions. J Chem Theory Comput 7:3995–4001

[36] Chai JD, Head-Gordon M (2008) Long-range corrected hybrid density functionals with damped atom–atom dispersion corrections. Phys Chem Chem Phys 10:6615–6620

[37] Frisch MJ, Trucks GW, Schlegel HB, et al (2016) Gaussian˜16 Revision C.01. Gaussian Inc. Wallingford CT

[38] Dunning THJ (1989) Gaussian basis sets for use in correlated molecular calculations. I. The atoms boron through neon and hydrogen. J Chem Phys 90:1007–1023

[39] Grimme S (2011) Density functional theory with london dispersion corrections. WIREs Comput Mol Sci 1:211–228

[40] Kozlowski D, Pilmé J (2011) New insights in quantum chemical topology studies using numerical grid-based analyses. J Comput Chem 32:3207–3217

[41] Chevreau H, Pilmé J (2023) Promising insights in parallel grid-based algorithms for quantum chemical topology. J Comput Chem 44:1505–1516

[42] Fievez T, Pinter B, Geerlings P, et al (2011) Regioselectivity in electrophilic aromatic substitution: Insights from interaction energy decomposition potentials. EurJOC 2011:2958–2968

[43] Frenking G, Loschen C, Krapp A, et al (2007) Electronic structure of co-an exercise in modern chemical bonding theory. J Comput Chem 28:117–126

[44] Yang T, Li Z, Wang XB, et al (2023) Quantitative descriptions of dewar-chatt-duncanson bonding model: A case study of zeise and its family ions. Chem Phys Chem 24:e202200835

[45] Alabugin IV, Kuhn L, Medvedev MG, et al (2021) Stereoelectronic power of oxygen in control of chemical reactivity: the anomeric effect is not alone. Chem Soc Rev 50:10253–10345

[46] Gould IR, Kollman PA (1994) Theoretical investigation of the hydrogen bond strengths in guanine-cytosine and adenine-thymine base pairs. J Am Chem Soc 116:2493–2499

[47] Nir E, Janzen C, Imhof P, et al (2002) Pairing of the nucleobases guanine and cytosine in the gas phase studied by ir–uv double-resonance spectroscopy and ab initio calculations. Phys Chem Chem Phys 4:732–739

[48] Bürgi HB, Dunitz JD, Lehn JM, et al (1974) Stereochemistry of reaction paths at carbonyl centres. Tetrahedron 30:1563–1572

[49] Bürgi HB, Dunitz JD, Shefter E (1973) Geometrical reaction coordinates. ii. nucleophilic addition to a carbonyl group. J Am Chem Soc 95:5065–5067

[50] Bürgi HB, Dunitz JD (1983) From crystal statics to chemical dynamics. Acc Chem Res 16:153–161

[51] Pilmé J, Berthoumieux H, Robert V, et al (2007) Unusual bond formation in aspartic protease inhibitors: A theoretical study. Chem Eur J 13:5388–5393

[52] Rodríguez HA, Bickelhaupt FM, Fernández I (2023) Origin of the bürgi-dunitz angle. Chem Phys Chem 24:e202300379

[53] Fujimoto H, Kato S, Yamabe S, et al (1974) Molecular orbital calculations of the electronic structure of borazane. J Chem Phys 60:572–578

[54] Loco D, Chataigner I, Piquemal JP, et al (2022) Efficient and accurate description of diels-alder reactions using density functional theory. Chem Phys Chem 23:e202200349

[55] Nicolaou KC, Snyder SA, Montagnon T, et al (2002) The diels-alder reaction in total synthesis. Angew Chem Int Ed 41:1668